

Dispersion-managed cnoidal pulse trainsYaroslav V. Kartashov,^{1,2} Victor A. Vysloukh,³ E. Marti-Panameño,^{1,4} David Artigas,¹ and Lluís Torner¹¹*ICFO-Institut de Ciències Fotoniques, and Department of Signal Theory and Communications, Universitat Politècnica de Catalunya, 08034 Barcelona, Spain*²*Chair of General Physics, Physics Department, M. V. Lomonosov Moscow State University, 119899, Vorobiovy Gory, Moscow, Russia*³*Departamento de Física y Matemáticas, Universidad de las Américas—Puebla, Santa Catarina Martir, CP 72820, Puebla, Cholula, Mexico*⁴*FCFM, Benemérita Universidad Autónoma de Puebla, Apdo Postal 1704, CP 72001, Puebla, Mexico*

(Received 5 May 2003; published 25 August 2003)

We report on the existence and properties of breathing periodic cnoidal pulse trains propagating in dispersion managed systems with piecewise constant dispersion. Our numerical investigations show that the dispersion management enhances the robustness of the periodic cnoidal pulse trains in comparison to the pulse trains existing in a uniform medium. The concept might have direct applications to pulse trains generated by mode-locked fiber lasers.

DOI: 10.1103/PhysRevE.68.026613

PACS number(s): 42.65.Jx, 42.65.Tg, 42.65.Wi

I. INTRODUCTION

Self-action and interaction of wave packets in nonlinear media with periodically varying dispersion or diffraction is a fundamental physical problem with a wide range of practical applications. Optical pulse transmission in dispersion-managed optical fibers (see, e.g., [1–10] and references therein), stretched pulse generation in mode-locked laser systems and recirculating fiber loops [11–16], propagation of guiding-center solitons and light bullets in tandem periodic quadratic nonlinear media [17,18], evolution of solitonlike beams in periodically modulated cubic nonlinear media [19,20] and in Bose-Einstein condensates [21,22] should be mentioned in this context.

During the last decade, impressive progress was achieved in this area from theoretical as well as experimental and practical points of view. Several methods have been developed to study the propagation of solitary nonlinear waves in dispersion or diffraction managed systems: different variational approaches [3,7,8,23–27], the guiding-center concept [1,5,9], the multiscale theory [28,29], spectral domain analysis [30], and the numerical averaging method [2,31,32]. In addition to conventional bright dispersion-managed solitons, dark, gray, and antisymmetric solitons were also studied recently [33–36]. Dispersion management offers a variety of advantages of paramount practical importance in high-bit-rate, long-haul optical fiber links. In this context, the key features of dispersion-managed systems employing so-called return-to-zero, or solitonlike pulse trains, are the reduced pulse-pulse interaction and the pulse energy enhancement, which are possible under proper conditions [37–42]. This reduces the inter-symbol-interaction errors and enhances the signal-to-noise ratio; hence dispersion-managed soliton pulse trains exhibit improved performances in data transmission communications. Thus, high-bit-rate, long-haul, all-optical fiber links employing this technique are already installed and in use.

Besides localized single-pulse solutions, the nonlinear

Schrödinger equation (NLS) that serves as a starting point for the description of many dispersion-managed systems admits periodic solutions in the form of Jacobi elliptic functions, which lead to so-called cn, dn, and sn waves that exist in different regimes characterized by a varying degree of localization. In the regime of strong localization, dn and cn waves feature, respectively, trains of in-phase or out-of-phase well-separated solitonlike pulses. Similarly, sn waves describe trains of out-of-phase dark solitons or optical kinks. In the case of weak localization, the cnoidal wave concept bridges the gap between soliton and linear harmonic (cn and sn cases) or continuous (dn case) waves. From this point of view, notice that periodic nonlinear waves play a similar role in nonlinear optics as diffraction gratings in classical linear optics. On the other hand, passive mode-locked fiber lasers under certain conditions can deliver a continuous wave train of picosecond or femtosecond pulses at a repetition rate higher than 100 GHz [11,12,14,16], with essentially discrete Fourier spectra of synchronized modes, which can be effectively described by cnoidal waves. The properties of stationary cnoidal waves supported by the NLS in uniform media have been studied in detail (see Refs. [43–47]). Nevertheless, the impact of dispersion management on the cnoidal wave pulse trains, hence the corresponding new features and practical advantages, have never been addressed to date.

In this paper, we report on the result of comprehensive computer simulations that reveal, for the first time to our knowledge, the existence and basic properties of whole families of breathing cnoidal waves in dispersion managed physical systems described by the NLS. In the strong localization limit, these waves have much in common with dispersion managed solitons. In particular, the energy of breathing cnoidal wave is enhanced relative to the pulse trains propagating in media with the corresponding constant average dispersion. We have shown that periodic dispersion modulation can strongly, yet not completely, reduce the dynamical and modulational instabilities that affect the families of cnoidal wave trains.

II. THEORETICAL MODEL AND SYSTEM PARAMETERS

Our starting point is the (1+1)-dimensional nonlinear Schrödinger equation for the lossless focusing cubic medium, modified to include spatially varying group velocity dispersion $d(\xi)$:

$$i \frac{\partial q}{\partial \xi} = \frac{1}{2} d(\xi) \frac{\partial^2 q}{\partial \eta^2} - q|q|^2. \quad (1)$$

Here $q(\eta, \xi) = (L_{\text{dis}}/L_{\text{spm}})^{1/2} A(\eta, \xi) I_0^{-1/2}$ is the dimensionless complex amplitude, $A(\eta, \xi)$ is the slowly varying envelope, I_0 is the input intensity, $\eta = (t - z/u_{\text{gr}})/\tau_0$ is the normalized running time, τ_0 is the characteristic time scale, $u_{\text{gr}} = (\partial k / \partial \omega)_{\omega=\omega_0}^{-1}$ is the group velocity, $k_0 = k(\omega_0)$ is the wave number, ω_0 is the carrying frequency, $\xi = z/L_{\text{dis}}$ is the normalized propagation distance, and $L_{\text{dis}} = \tau_0^2 / |\beta_2|$ is the dispersion length. The coefficient $\beta_2 = (\partial^2 k / \partial \omega^2)_{\omega=\omega_0}$ is defined by the group velocity dispersion (GVD) for a standard telecommunication fiber, $L_{\text{spm}} = 2c / (\omega_0 n_2 I_0)$ is the self-phase modulation length, and $n_2 = 3\pi\omega_0 \chi^{(3)}(\omega_0) / [k(\omega_0)c]$ is the nonlinear coefficient which is proportional to the Fourier transform $\chi^{(3)}(\omega_0)$ of the corresponding element of the nonlinear susceptibility tensor.

Throughout the paper we consider the simplest two-step dispersion map consisting of two fiber segments with lengths L_a and L_n , having different GVD coefficients $\beta_{a,n}$ at the carrier frequency ω_0 . Therefore the dimensionless dispersion coefficient in Eq. (1) is introduced as

$$\begin{aligned} d(\xi) &= d_a \quad \text{for } nL \leq \xi < nL + L_a/2, \\ d(\xi) &= d_n \quad \text{for } nL + L_a/2 \leq \xi < nL + L_a/2 + L_n, \\ d(\xi) &= d_a \quad \text{for } nL + L_a/2 + L_n \leq \xi < (n+1)L, \end{aligned} \quad (2)$$

where $L = L_a + L_n$ is the period of the dispersion map, $n = 0, 1, 2, \dots$, and $d_a = \beta_a / |\beta_2| < 0$ and $d_n = \beta_n / |\beta_2| > 0$ for fiber segments with anomalous and normal group velocity dispersion, respectively. We assume that light is launched into the fiber in the middle of the segment with anomalous GVD, corresponding to one of the chirp-free points of the system. Note that for the typical value $|\beta_2| = 0.2 \text{ ps}^2/\text{km}$ of the GVD coefficient for telecommunication fibers and the typical pulse width $\tau_0 = 1 \text{ ps}$, the period of the dispersion map $L = 1$ that is used in the paper corresponds to an actual propagation distance of about 5 km. For simplicity, from now on we consider dispersion maps with equal lengths of fiber segments with anomalous and normal GVD, i.e., $L_a = L_n = L/2$.

The two-step dispersion map considered here is fully characterized by two parameters: the path-average dispersion $d_{\text{ave}} = (d_a L_a + d_n L_n) / L$ and the dispersion modulation depth $\delta d = d_n - d_a$. For the constant anomalous group velocity dispersion $d(\xi) \equiv -1$, Eq. (1) admits two periodic stationary solutions in the form of cnoidal dn and cn waves [43–47], given by

$$\begin{aligned} q_{\text{dn}}(\eta, \xi) &= \chi \text{dn}[\chi(\eta - \eta_0 - \alpha\xi), m] \exp[i\alpha\eta + i\xi\chi^2] \\ &\times (1 - m^2/2) - (i/2)\alpha^2\xi + i\psi_0], \end{aligned}$$

$$\begin{aligned} q_{\text{cn}}(\eta, \xi) &= m\chi \text{cn}[\chi(\eta - \eta_0 - \alpha\xi), m] \exp[i\alpha\eta + i\xi\chi^2] \\ &\times (m^2 - 1/2) - (i/2)\alpha^2\xi + i\psi_0], \end{aligned} \quad (3)$$

and one stationary periodic solution for normal constant dispersion $d(\xi) \equiv 1$:

$$\begin{aligned} q_{\text{sn}}(\eta, \xi) &= m\chi \text{sn}[\chi(\eta - \eta_0 - \alpha\xi), m] \exp[-i\alpha\eta \\ &+ i\xi\chi^2(1 + m^2)/2 + (i/2)\alpha^2\xi + i\psi_0]. \end{aligned} \quad (4)$$

In expressions (3) and (4), the symbols $\text{cn}(\eta, m)$, $\text{dn}(\eta, m)$, and $\text{sn}(\eta, m)$ stand for elliptic functions, $0 \leq m \leq 1$ is the modulus of the elliptic function that can be treated as a parameter describing the degree of localization of the wave field energy, χ is the arbitrary form factor, η_0 is the initial time shift, α is the initial frequency shift, and ψ_0 is the initial phase. Note that the period of the dn wave is $2K(m)/\chi$, where $K(m)$ is the elliptic integral of the first kind, whereas the period of both the cn waves and the sn waves is $4K(m)/\chi$, which is twice higher.

In the case of weak dispersion maps, i.e., $\delta d \ll 1$, one can average Eq. (1) over large propagation distances ξ to obtain a system with constant coefficients. The solutions of this equation also have the form of Eqs. (3) and (4) and can serve as a good initial guess for the calculation of the profile of the true breathing cnoidal waves propagating in stronger maps, with higher values of dispersion modulation depth δd , when direct averaging is inapplicable. It is instructive to rescale the resulting solution of Eqs. (3) and (4) by the proper selection of the form factor χ , in such way that the period T of the dn wave equals to 2π and the period of the cn and sn wave equals to 4π . This choice means that the characteristic time scale τ_0 in Eq. (1) is related to the repetition rate of pulses in the cnoidal wave train but not to the individual pulse duration.

To find the profiles of the arbitrary dispersion-managed cnoidal waves, we used the method of numerical averaging developed by Nijhof and co-workers [2,31,32]. Convergence of this method proved to be relatively fast for well-localized solitonlike high-energy solutions and is considerably slower for delocalized low-energy quasiharmonic waves. For strong dispersion maps, the propagation distance step should be carefully controlled in the calculations to avoid numerical errors.

The profiles of the numerically calculated breathing cnoidal waves are generally nontrivial, and can be characterized by two key parameters, namely, the energy flow U per time period T ,

$$U = \int_{-T/2}^{T/2} |q(\eta, \xi)|^2 d\eta, \quad (5)$$

and the integral width of the individual pulses forming the periodic sequence, defined as

$$W = 2 \left(\int_{-T/4}^{T/4} \eta^2 |q(\eta, \xi)|^2 d\eta \right)^{1/2} \left(\int_{-T/4}^{T/4} |q(\eta, \xi)|^2 d\eta \right)^{-1/2}. \quad (6)$$

This expression is valid only for cnoidal cn waves and sn waves, whereas in the case of dn waves integration in Eq. (6) should be carried out over the segment $[-T/2, T/2]$. The energy flow (5) gives a measure of the strength of the nonlinearity and the integral width (6) determines the *degree of localization of the energy flow carried by the pulses of the cnoidal wave*. For the fixed cnoidal wave period T , the integral width W can be treated as a function of U . Hence, the dependencies $W(U)$ for periodic waves in dispersion-managed fiber links are somehow analogous to the dispersion curves (dependencies of energy flow on nonlinearity induced phase shift) for localized stationary solitons in the uniform NLS. We thus use the dependencies $W(U)$ to characterize the whole families of dispersion-managed cnoidal waves.

III. RESULTS AND DISCUSSION

Using the numerical averaging method described above, we have analyzed the basic properties of the cn-, dn-, and sn-type breathing cnoidal waves existing for different values of the path-average dispersion d_{ave} and dispersion modulation depth δd . The period of the cn and sn waves was set to 4π , whereas the period of dn wave was set to 2π . Solutions for arbitrary values of these periods can be obtained from the above cases by simple scaling transformations using the similarity rules of the NLS.

cn-type breathing wave. The typical propagation dynamics of cn waves is shown in Fig. 1 for low and high values of the energy flow, in the case of anomalous path-average dispersion and a relatively strong dispersion map. For this dispersion map there exist two chirp-free points (where local frequency $d\varphi/d\eta \equiv 0$) situated in the middle of segments with normal and anomalous GVD, and two points with maximal chirp situated at the boundaries between segments with normal and anomalous GVD. In the first part of the anomalous dispersion segment, spreading dominates over self-compression. After this, chirped wave enters normal dispersion segment, where it first compresses and then decompresses. Finally, the initial chirp-free profile is restored at the end of the second half of the anomalous dispersion segment. The intensity profile of low energy waves is almost harmonic. The frequency chirp at the entrance of the normal dispersion segment can also be approximated by a harmonic function shifted by a quarter of its period in comparison with the intensity distribution. The profile of high-energy waves looks like a sequence of well-separated bell-shaped pulses; the frequency chirp can be approximated by an elliptical function. However, in the central energy bearing part of the pulse, the frequency chirp is practically linear, a finding which is consistent with previous results on single solitons in dispersion-managed fiber links [1–10]. An interesting point is that the breathing of the high-energy wave is more pronounced [compare Figs. 1(a) and 1(b)].

Figure 2 summarizes the basic properties of cn waves. Figures 2(a) and 2(b) illustrate the energy-width diagrams $W(U)$ for different values of the dispersion modulation depth δd and path-average dispersion d_{ave} . It should be pointed out that for fixed pulse width and wave period, the

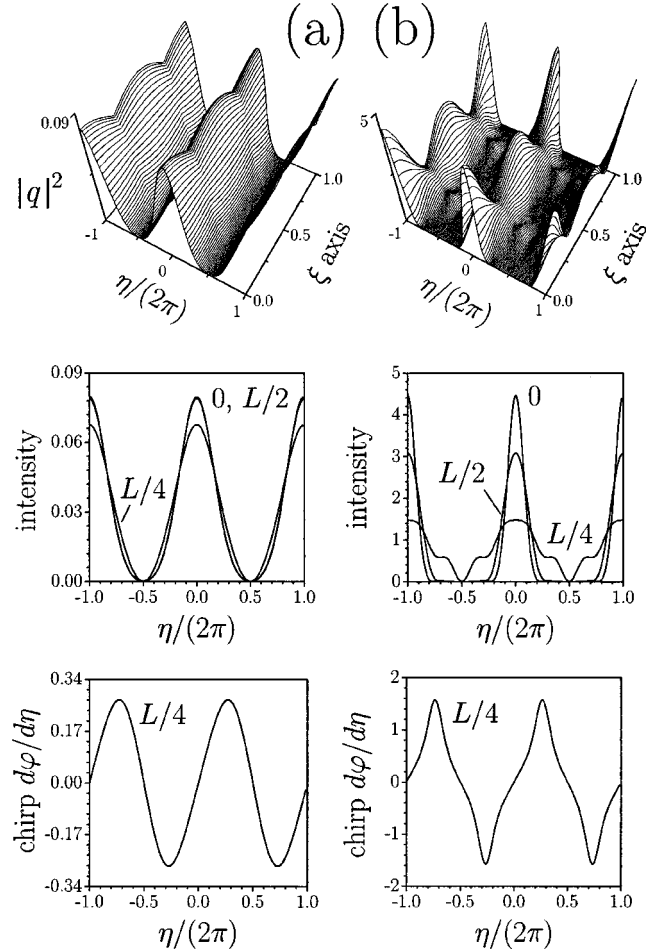


FIG. 1. Dynamics of propagation of cn waves with energy flows $U=0.4$ (a) and 10 (b) within one period of dispersion map. Conditions: $d_{\text{ave}} = -0.1$ and $\delta d = 10$. Lower plots display the intensity distribution and frequency chirp of the propagating waves at various distances. All quantities are plotted in dimensionless units.

energy flow of the cnoidal waves quickly increases with increase of the dispersion map strength (dispersion modulation depth), similar to the case of single dispersion-managed solitons. One can also see from Fig. 2(b) that for fixed width W , the energy flow increases with growing path-averaged dispersion modulus $|d_{\text{ave}}|$. This effect is most pronounced for small values of $|d_{\text{ave}}| \leq 0.2$. It should be pointed out that cn waves exist for zero value of path-average dispersion, and even for small positive values of d_{ave} , but in this parameter range the method of numerical averaging becomes unstable and it is difficult to obtain energy-width diagrams for the whole energy range. Typical profiles of cn waves are depicted in the Fig. 2(c) for different values of the energy flow U . One can see from this figure that with increasing energy flow, the wave transforms from an almost harmonic profile to a sequence of well-separated out-of-phase pulses with bell-like shapes. Further increase of the energy flow leads to appearance of oscillating tails in the pulses forming the cnoidal wave train. The presence of oscillating tails is also a characteristic feature of the dispersion-managed waves.

dn-type breathing wave. The propagation dynamics of the

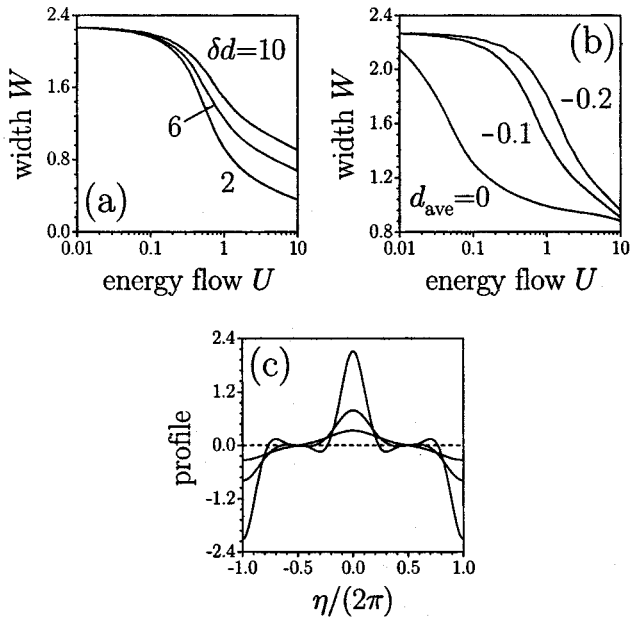


FIG. 2. Energy-width diagrams for the family of cn waves. (a) $d_{\text{ave}} = -0.1$ and various values of dispersion difference; (b) $\delta d = 10$ and various values of path-average dispersion d_{ave} . Panel (c) shows the wave profiles corresponding to the energy flows $U = 0.5, 2,$ and 10 , with $d_{\text{ave}} = -0.1$ and $\delta d = 10$. All quantities are plotted in dimensionless units.

dn waves is shown in Fig. 3 for the case of anomalous path-average dispersion. The main features of dn-wave propagation are similar to those encountered for cn waves. The main difference between these two waves is that dn waves in the low-energy limit contain a constant pedestal, whereas in the high-energy limit they transform into a sequence of in-phase solitons. As in the case of cn waves, the frequency chirp of low-energy dn waves at the boundary between segments with anomalous and normal dispersion can be described by harmonic functions. However, in the high-energy limit, the frequency chirp profile is more complicated. In the central part of the pulse, the chirp remains almost linear.

Typical features of the families of dn waves are summarized in Fig. 4. Figures 4(a) and 4(b) show energy-width diagrams $W(U)$ for different values of the dispersion modulation depth δd and path-average dispersion d_{ave} . These dependencies differ from those of cn waves only in the low-energy limit $U \ll 1$ where the contribution of the constant pedestal is considerable. At fixed width W , the energy flow of the breathing dn waves increases with growing dispersion map strength (dispersion modulation depth). One can also see a drastic increase of the energy flow of the dn waves for fixed width, with increase of the modulus of the path-average dispersion $|d_{\text{ave}}|$ [Fig. 4(b)]. Notice that this effect is most pronounced for weakly localized waves with relatively high widths $W \sim 2$. Representative profiles of the dn-type cnoidal waves are shown in the Fig. 4(c) for different values of the energy flow U . When increasing the energy flow, the dispersion-managed dn-wave transforms from harmonic oscillations superimposed on constant pedestal into a sequence of bell-shaped in-phase solitons that acquire oscillating tails

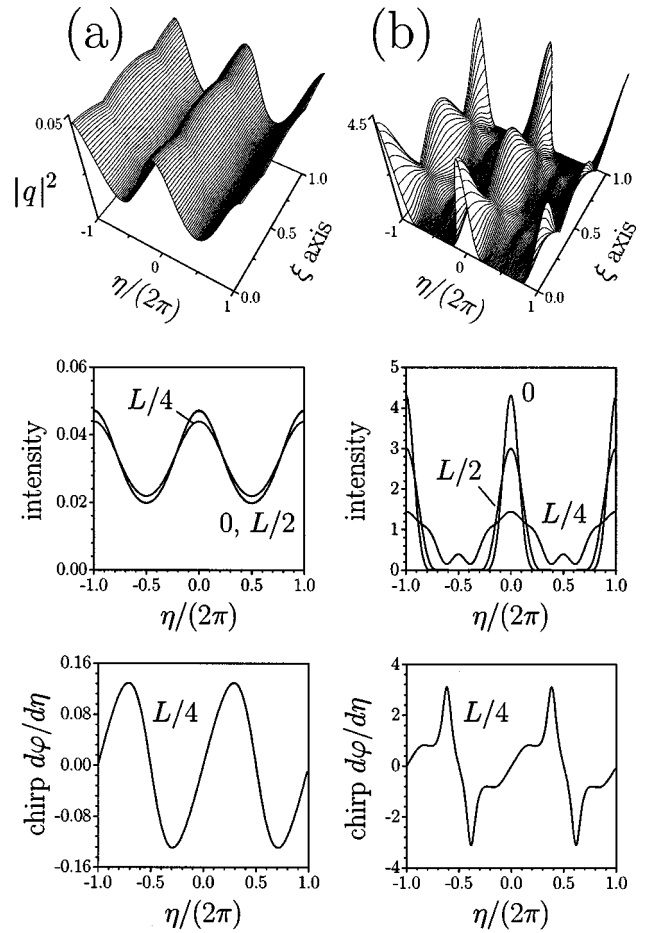


FIG. 3. Dynamics of propagation of dn waves with energy flows $U = 0.2$ (a) and 5 (b) within one period of dispersion map. Conditions: $d_{\text{ave}} = -0.1$ and $\delta d = 10$. Lower plots display the intensity distribution and frequency wave chirp at various propagation distances. All quantities are plotted in dimensionless units.

for high enough U values. Also note that contrary to its counterpart in the NLS with constant dispersion, the dn waves in dispersion-managed system can change sign along the temporal coordinate η .

sn-type breathing waves. We have found waves of this type only at the regime of normal path-average group velocity dispersion, i.e., $d_{\text{ave}} > 0$. Figure 5 illustrates the propagation dynamics of sn waves inside one period of the dispersion map. It should be mentioned that for the same value of the dispersion modulation depth, the intensity variations for the sn wave are rather weak in comparison with those encountered for cn and dn waves. The profile of low-energy sn waves is very close to the quasilinear harmonic wave; the frequency chirp at the boundary between segments with anomalous and normal dispersions can be well described by a harmonic function in the low-energy limit. High-energy waves exhibit rather complicated intensity profiles (see also Fig. 6 with the properties of sn-wave families), but have much in common with the sequence of out-of-phase dark solitons. Notice that dispersion-managed sn waves have pronounced amplitude oscillations in the plateau area, in contrast with conventional snoidal waves in the NLS with con-

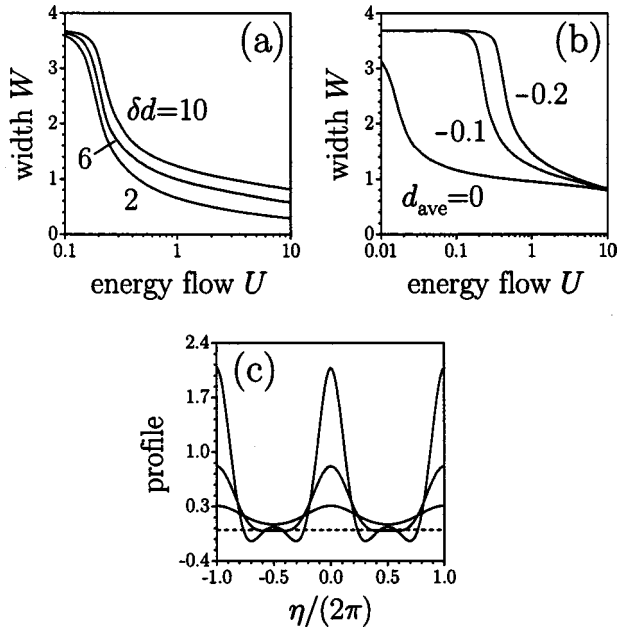


FIG. 4. Energy-width diagrams for the family of dn waves. (a) $d_{\text{ave}} = -0.1$ and various values of dispersion difference; (b) $\delta d = 10$ and various values of path-average dispersion d_{ave} . Panel (c) shows the wave profiles corresponding to energy flows $U = 0.25, 1,$ and 5 , with $d_{\text{ave}} = -0.1$ and $\delta d = 10$. All quantities are plotted in dimensionless units.

stant dispersion. Such oscillations were recently shown to be the characteristic feature of strongly dispersion-managed dark solitons [36]. The frequency chirp in the plateau area is almost linear. As one can see from the Fig. 6, the width of the pulses carried by sn waves is a nonmonotonic function of the energy flow. We attribute this specific feature to pronounced oscillations of the wave amplitude in the plateau area that grows up with increase of energy flow [Fig. 6(c)]. Notice that sn-type cnoidal wave looks like a sequence of kinks up to moderate values of energy flow, a feature that might find practical applications.

Cnoidal waves in media with constant dispersion are known to be unstable with respect to the perturbations of input profiles in the anomalous dispersion regime and stable in the normal dispersion regime [43–47]. Thus, dn waves are highly unstable due the presence of constant background, whereas cn waves suffer weak oscillatory instabilities; sn waves are completely stable in normal dispersion. Therefore, the natural question that arises is whether the influence of alternating dispersion in different segments of dispersion map reduces the instability strength of the cnoidal pulse trains. To get insight into this issue, we have solved the governing Eq. (1) numerically with the input conditions $q(\eta, \xi = 0) = w(\eta)F(\eta)[1 + \rho(\eta)]$, where $w(\eta)$ is the profile of the breathing dispersion-managed waves, $\rho(\eta)$ is a complex random function with a Gaussian distribution and variance σ^2 , and $F(\eta)$ is a broad Gaussian envelope imposed on the otherwise transversely infinite pulse pattern. The width of the envelope was much bigger than the cnoidal wave period and we monitored the evolution dynamics in the central part of the envelope.

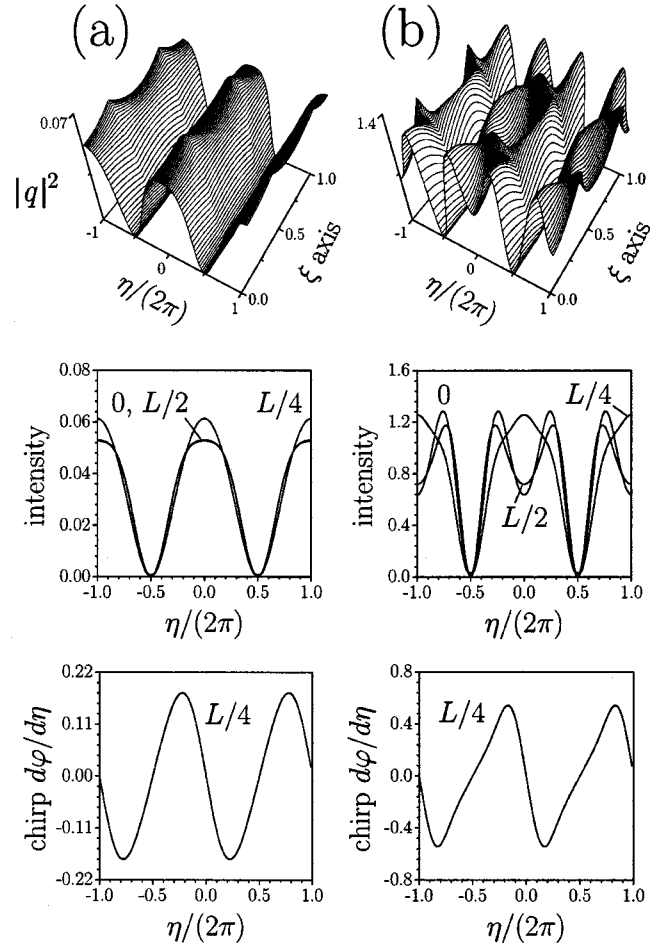


FIG. 5. Dynamics of propagation of sn waves with energy flows $U = 0.4$ (a) and 10 (b) within one period of dispersion map. Conditions: $d_{\text{ave}} = 0.1$ and $\delta d = 10$. Lower plots display the intensity distribution and frequency wave chirp at various propagation distances. All quantities are plotted in dimensionless units.

The typical propagation dynamics of perturbed dispersion-managed cn waves with moderate width $W = 1.24$ and energy flow $U = 2$ is shown in Fig. 7(a). One can see that dispersion-managed waves conserve their input structure for large distances (in the particular case displayed, up to 250 dispersion lengths). The instability of the cn waves decreases with growing energy flows (i.e., at higher degree of localization). For example, we observed numerically that the perturbed cn waves with energy flow $U = 20$ could propagate undistorted over more than 1000 dispersion lengths. This result could be compared with propagation of perturbed cnoidal waves in uniform medium. Comparison can be made with different criteria, e.g., one can follow the dynamics of perturbed waves with the same energy flow or with the same width. Moreover, it is possible to consider uniform medium either with dispersion coefficient d corresponding to path-average dispersion d_{ave} or with dispersion coefficient corresponding to dispersion d_a on the anomalous segment of fiber link. A cn wave in an uniform medium with $d = d_{\text{ave}}$

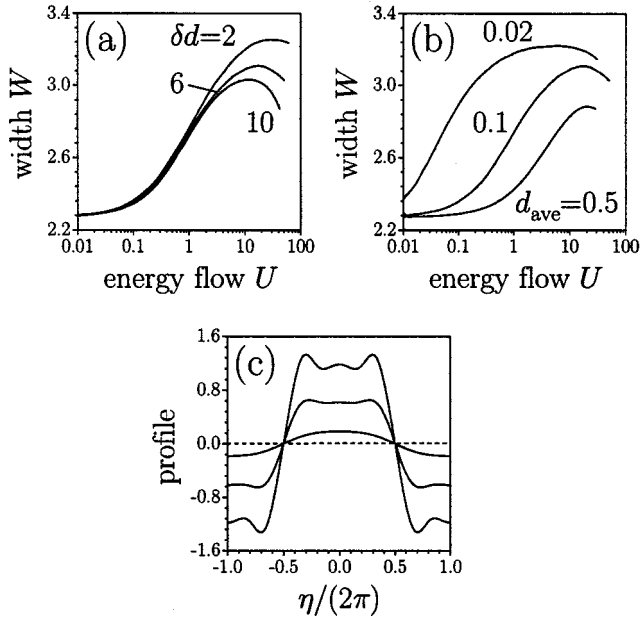


FIG. 6. Energy-width diagrams for the families of sn waves. (a) $d_{\text{ave}}=0.1$ and various values of dispersion difference; (b) $\delta d=6$ and various values of path-average dispersion d_{ave} . Panel (c) shows the wave profiles corresponding to the energy flows $U=0.25, 4$, and 15 , with $d_{\text{ave}}=0.1$ and $\delta d=6$. All quantities are plotted in dimensionless units.

and the same energy flow is much more localized than its dispersion-managed counterpart. Despite this fact, the corresponding cn wave in the uniform medium destabilizes much faster than the dispersion-managed cn wave. A typical example is shown in Fig. 7(b). In contrast, for this particular case, the cnoidal wave in the uniform medium with $d=d_{\text{ave}}$ and with the same individual pulse width survives larger propagation distances than its dispersion-managed counterpart. This is illustrated in Fig. 7(c). Note, however, that the corresponding wave in the uniform medium carries an extremely low energy, and thus is close to a linear harmonic wave. Note that such stabilization of cnoidal waves in the low-energy limit is a known fact [43–47]. However, such waves are not attractive from a practical point of view because of their low contrast, hence very small signal-to-noise ratio. The comparison of the propagation dynamics of perturbed dispersion-managed waves and waves in uniform medium with $d=d_a$ with equal energies and equal widths [Figs. 7(d) and 7(e), respectively] also leads to the conclusion that dispersion-managed waves feature weaker instabilities. On physical grounds, such stabilization is analogous to the reduction of the time jitter of isolated pulses in dispersion-managed fiber transmission lines with strong maps. This conclusion holds also for the case of dn waves with moderate and high energies $U>1$, when the constant pedestal almost vanishes and thus the modulational instability is correspondingly weakened. Finally, notice that sn waves which are completely stable in uniform medium with normal dispersion become unstable in dispersion-managed fibers. However, in

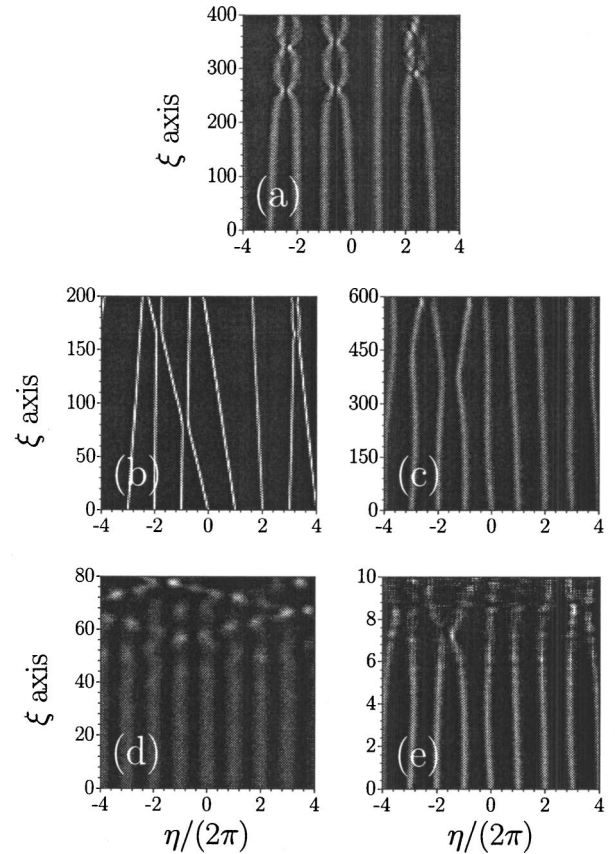


FIG. 7. (a) Dynamics of propagation of the perturbed dispersion-managed cn wave with width $W=1.24$ and energy flow $U=2$, with $d_{\text{ave}}=-0.1$, $\delta d=10$. For comparison, (b) and (c) show the dynamics of propagation of the perturbed stationary wave with the same energy and the same width, respectively, but in the uniform medium with dispersion $d=-0.1$ equal to path-average dispersion d_{ave} . Panels (d) and (e) show the propagation of perturbed stationary wave with, respectively, the same energy and width as for wave (a), but in uniform medium with dispersion $d=-5.1$ (i.e., the dispersion on anomalous segment of dispersion map). Random noise realizations are identical in all cases. Noise variance $\sigma^2=0.02$. All quantities are plotted in dimensionless units.

our simulations, as in the case of cn waves, the typical decay distance for sn waves exceeds 100–200 dispersion lengths.

IV. CONCLUSIONS

In summary, we have found numerically families of dispersion-managed, breathing cnoidal wave trains of cn, dn, and sn types supported by NLS models. Such wave trains are energy enhanced in comparison with their counterparts in uniform settings with the same average dispersion. In the case of pulse trains propagating in optical fibers, this is favorable from the practical point of view because it yields an improved signal-to-noise ratio. We also found that under proper conditions, dispersion management enhances the dynamical stability and reduces the time jitter of the cnoidal wave trains.

ACKNOWLEDGMENTS

Financial support from CONACyT under Grant No. U39681-F is gratefully acknowledged by V.A.V. Y.V.K. and

L.T. acknowledge support by the Generalitat de Catalunya and by the Spanish Government under Contract No. BFM2002-2861. E.M.P. thanks CONACyT–Mexico for support within the framework of the program Estancias Sabáticas en Instituciones del Extranjero.

-
- [1] A. Hasegawa and Y. Kodama, *Opt. Lett.* **16**, 1385 (1991).
 [2] J. H. B. Nijhof, N. J. Doran, W. Forysiak, and F. M. Knox, *Electron. Lett.* **33**, 1726 (1997).
 [3] E. G. Shapiro and S. K. Turitsyn, *Opt. Lett.* **22**, 1544 (1997).
 [4] A. Bernston, N. J. Doran, W. Forysiak, and J. H. B. Nijhof, *Opt. Lett.* **23**, 900 (1998).
 [5] Y. Kodama, *Physica D* **123**, 255 (1998).
 [6] S. K. Turitsyn and E. G. Shapiro, *Opt. Lett.* **23**, 682 (1998).
 [7] T. I. Lakoba, J. Yang, D. J. Kaup, and B. A. Malomed, *Opt. Commun.* **149**, 366 (1998).
 [8] V. S. Grigoryan and C. R. Menyuk, *Opt. Lett.* **23**, 609 (1998).
 [9] A. Hasegawa, *IEEE J. Sel. Top. Quantum Electron.* **6**, 1161 (2000).
 [10] M. Nakazawa, A. Sahara, and H. Kubota, *J. Opt. Soc. Am. B* **18**, 409 (2001).
 [11] T. Silvestre, S. Coen, P. Emplit, and M. Haelterman, *Opt. Lett.* **27**, 482 (2002).
 [12] C. J. S. Matos, D. A. Chestnut, and J. R. Taylor, *Opt. Lett.* **27**, 915 (2002).
 [13] H. Haus, *IEEE J. Sel. Top. Quantum Electron.* **6**, 1173 (2000).
 [14] R.-M. Mu, V. S. Grigoryan, and C. R. Menyuk, *IEEE J. Sel. Top. Quantum Electron.* **6**, 248 (2000).
 [15] M. Matsumoto, *Opt. Lett.* **22**, 1238 (1997).
 [16] P. Franco, F. Fontana, I. Cristiani, M. Midrio, and M. Romagnoli, *Opt. Lett.* **20**, 2009 (1995).
 [17] L. Torner, *Opt. Lett.* **23**, 1256 (1998); *IEEE Photonics Technol. Lett.* **11**, 1268 (1999).
 [18] L. Torner, S. Carrasco, J. P. Torres, L.-C. Crasovan, and D. Mihalache, *Opt. Commun.* **199**, 277 (2001).
 [19] L. Berge, V. K. Mezentsev, J. J. Rasmussen, P. L. Christiansen, and Yu. B. Gaididei, *Opt. Lett.* **25**, 1037 (2000).
 [20] I. Towers and B. Malomed, *J. Opt. Soc. Am. B* **19**, 537 (2002).
 [21] F. Kh. Abdullaev, J. G. Caputo, R. A. Kraenkel, and B. A. Malomed, *Phys. Rev. A* **67**, 013605 (2003).
 [22] H. Saito and M. Ueda, *Phys. Rev. Lett.* **90**, 040403 (2003).
 [23] S. K. Turitsyn, I. Gabitov, E. W. Laedke, V. K. Mezentsev, S. L. Musher, E. G. Shapiro, T. Schafer, and K. H. Spatschek, *Opt. Commun.* **151**, 117 (1998).
 [24] F. Kh. Abdullaev and J. G. Caputo, *Phys. Rev. E* **58**, 6637 (1998).
 [25] H. A. Haus and Y. Chen, *J. Opt. Soc. Am. B* **16**, 889 (1999).
 [26] S. K. Turitsyn, A. B. Aceves, C. K. R. T. Jones, and V. Zharnitsky, *Phys. Rev. E* **58**, R44 (1998).
 [27] S. K. Turitsyn, N. F. Smyth, and E. G. Turitsyna, *Phys. Rev. E* **58**, R48 (1998).
 [28] M. J. Ablowitz and G. Biondini, *Opt. Lett.* **23**, 1668 (1998).
 [29] V. Cauteraerts, M. Akihino, and Y. Kodama, *Chaos* **10**, 515 (2000).
 [30] C. Pare and P.-A. Belanger, *Opt. Lett.* **25**, 881 (2000).
 [31] N. J. Smyth, N. J. Doran, W. Forysiak, and F. M. Knox, *J. Lightwave Technol.* **15**, 1808 (1997).
 [32] J. H. B. Nijhof, W. Forysiak, and N. J. Doran, *IEEE J. Sel. Top. Quantum Electron.* **6**, 330 (2000).
 [33] Y. Chen, *Opt. Commun.* **161**, 267 (1999).
 [34] C. Pare and P.-A. Belanger, *Opt. Commun.* **168**, 103 (1999).
 [35] A. Maruta, T. Inoue, Y. Nonaka, and Y. Yoshika, *IEEE J. Sel. Top. Quantum Electron.* **8**, 640 (2002).
 [36] M. J. Ablowitz and Z. H. Musslimani, *Phys. Rev. E* **67**, 025601(R) (2003).
 [37] P. V. Mamyshev and L. F. Mollenauer, *Opt. Lett.* **24**, 448 (1999).
 [38] Y. Chen and H. A. Haus, *Opt. Lett.* **24**, 217 (1999).
 [39] M. J. Ablowitz, G. Biondini, and E. S. Olson, *Opt. Lett.* **18**, 577 (2001).
 [40] M. J. Ablowitz and T. Hirooka, *Opt. Lett.* **25**, 1750 (2000).
 [41] P. Johansson, D. Anderson, M. Marklund, A. Bernston, M. Forzati, and J. Martensson, *Opt. Lett.* **27**, 1073 (2002).
 [42] C. Xu, C. Xie, and L. Mollenauer, *Opt. Lett.* **27**, 1303 (2002).
 [43] V. Aleshkevich, V. Vysloukh, and Y. Kartashov, *Opt. Commun.* **173**, 277 (2000).
 [44] V. Aleshkevich, Y. Kartashov, and V. Vysloukh, *Opt. Commun.* **185**, 305 (2000).
 [45] V. Aleshkevich, Y. Kartashov, and V. Vysloukh, *J. Opt. Soc. Am. B* **18**, 1127 (2001).
 [46] V. A. Aleshkevich, V. A. Vysloukh, and Y. V. Kartashov, *Quantum Electron.* **31**, 257 (2001).
 [47] Y. V. Kartashov, V. A. Aleshkevich, V. A. Vysloukh, A. A. Egorov, and A. S. Zelenina, *Phys. Rev. E* **67**, 036613 (2003).